

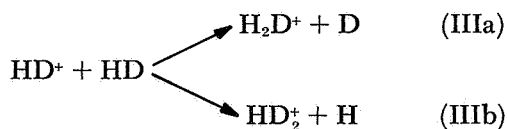
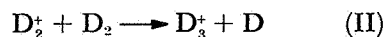
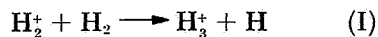
XIII. Physics

SPACE SCIENCES DIVISION

A. An Ion Cyclotron Resonance Study of the Energy Dependence of the Ion-Molecule Reaction in Gaseous HD, D. D. Elleman,

J. King, Jr., and M. T. Bowers

The ion cyclotron resonance (ICR) spectrometer is a relatively new instrument used in the study of ion-molecule reactions (Refs. 1-4). Whenever possible, it is important to compare these early ICR results with both theoretical predictions and results obtained by more conventional techniques. The following ion-molecule reactions in gaseous hydrogen were the subjects of an ICR study at JPL:



These reactions were chosen because of the rather extensive theoretical work performed on the reaction cross sections (Ref. 5). Comparisons can also be made between

the ICR data and the results obtained by the more conventional techniques, i.e., high-pressure mass spectroscopy (Refs. 6 and 7), tandem mass spectroscopy (Refs. 8 and 9), and merged beam spectroscopy (Ref. 10).

Both ICR and ion cyclotron double resonance (ICDR) techniques have been used to study the energy dependence of the rate constants of reactions I and II (Ref. 11). In these studies, it became apparent that a more careful determination of the reactant ion energy would be needed. This article describes how the average reactant ion energy in an ICDR experiment can be calibrated using the ratio $\text{H}_2\text{D}^+/\text{HD}_2^+$ versus the energy data of J. H. Futrell and F. P. Abramson (Ref. 9). The value of the ratio observed in ICDR experiments at various settings of the irradiating field strength $E = E_0 \sin \omega t$ is then compared with the ratio given in Ref. 9.

The ICDR ratio was obtained in the following manner: The HD gas was placed in the ICR cell [2.5 cm (trapping field) \times 2.1 cm (irradiating field)] and was slightly ionized with a 30-eV electron beam. The H_2D^+ and HD_2^+ resonance lines resulting from reactions IIIa and IIIb were observed with the pulsed-drift-voltage mode of operation (Ref. 3), while the HD^+ resonance line was irradiated

with the second RF oscillator. The intensity of the HD_2^+ line was corrected for its different extent of reaction by multiplying its intensity by 4/5 (Ref. 12). Corrections for the line intensities had to be made since the second RF irradiating electric field heated the ion in the observing section of the cell only, and not in the source region. The observing section of the cell was 5.08 cm long, and the source region where reaction could also take place was 2.54 cm long. Therefore, $\frac{1}{3}$ of the intensity of the secondary line was due to thermal reactions that occurred in the source region of the cell. The corrected intensity of the H_2D^+ ion is then given by

$$\text{H}_2\text{D}^+ I_c = \text{H}_2\text{D}^+ I_m - \frac{1}{3} \text{H}_2\text{D}^+ I_m^0 \quad (1)$$

where $\text{H}_2\text{D}^+ I_m$ is the uncorrected measured intensity of the H_2D^+ ion when the HD^+ ion is heated by double resonance, and $\text{H}_2\text{D}^+ I_m^0$ is the measured intensity of the H_2D^+ ion when it is produced by thermal HD^+ ions only. A similar expression gives the corrected intensity for the HD_2^+ ion:

$$\text{HD}_2^+ I_c = \frac{4}{5} \text{HD}_2^+ I_m - \frac{1}{3} \text{HD}_2^+ I_m^0 \quad (2)$$

where the $\frac{4}{5}$ factor takes into account the difference in the extent of reaction for H_2D^+ and HD_2^+ ions. This correction factor is the ratio of the H_2D^+ and HD_2^+ masses, or the ratio of the magnetic field values that satisfies the resonance conditions in the field-sweep mode of operation. These corrected intensities were then used to give the ratio $\text{H}_2\text{D}^+/\text{HD}_2^+$ in Table 1. Also given in Table 1 are the electric field strength of the second RF oscillator used to heat the primary ions and the laboratory kinetic energy of the ions obtained by comparing the ratio $\text{H}_2\text{D}^+/\text{HD}_2^+$ to the data of Ref. 9. The fields reported are 80% of those at the plates in the resonance region. (A complete discussion of the electric field profiles can be found in Ref. 13.)

As a further comparison, the energy of the primary ion was determined by two additional methods. For the first, it was assumed that, if the ion energy is limited by collisions, the average ion energy can be estimated by measuring the linewidth at a known value of the electric field strength of the observing oscillator. The average ion energy can then be calculated using (Refs. 14 and 15)

$$E_{\text{ion}} = \frac{1}{2} KT + \frac{q^2 E^2 (m_p + M)}{\delta \xi_p^2 M_p} \quad (3)$$

where M is the mass of the neutral species relaxing the ion momentum, m_p is the mass of the primary ion, E is

Table 1. Observed $\text{H}_2\text{D}^+/\text{HD}_2^+$ ratio at various ICDR irradiating field strengths

$\text{H}_2\text{D}^+/\text{HD}_2^+$	E_0 , V/m	Laboratory kinetic energy, eV		
		Calibration data ^a	Linewidth data ^b	Drift time data ^c
0.73	0	~0	—	—
0.83	1.1	0.2	0.12	0.6
0.89	1.6	0.4	0.20	1.3
0.93	2.0	0.5	0.27	2.0
0.95	2.6	0.6	0.30	3.5
0.95	3.2	0.6	0.36	5.3
0.98	4.0	0.8	0.48	8.3
1.01	5.0	0.9	0.58	13.2
1.02	6.2	1.0	0.68	20.4
1.05	8.0	1.2	0.87	33.2
1.09	10.0	1.4	1.12	51.0
1.16	12.4	1.6	1.33	80.0
1.17	16.0	1.7	1.46	133.0
1.18	20.0	1.7	1.75	215.0
1.19	25.8	1.8	2.16	320.0
1.23	31.1	2.0	2.60	505.0

^aExtracted from Fig. 8 in Ref. 9, using the ratios in column 1. The error in the extraction is of the order of $\pm 10\%$.
^bCalculated from Eq. (19) in Ref. 12 and the experimental ICDR linewidths.
^cCalculated from Eq. (20) in Ref. 12, with the drift time τ calculated from the resonance region voltage. A value of $\tau/2$ was used to calculate the energies reported here.

the irradiating field strength, ξ_p is the collision frequency related to the line width, and $\frac{1}{2} KT$ is the thermal energy of the ion. The fourth column in Table 1 gives the results obtained using this method of analysis.

For the second additional comparison, it was assumed that the ion energy is limited by the amount of time the ion is exposed to the irradiating field. In the low collision limit, the ion is exposed to the irradiating field during the time, τ , that it takes the ion to drift through the observing region of the ICR cell. Under these conditions, the energy of the ion is given by (Refs. 14 and 15)

$$E_{\text{ion}} = \frac{q^2 E^2 \tau^2}{\delta m_p} \quad (4)$$

The fifth column in Table 1 gives the results of using this approach. It is evident that the collision-limited energies calculated from ICDR linewidths are of the proper order of magnitude, while the drift time energy estimates are grossly exaggerated. The zero irradiating field value of the ICR ratio $\text{H}_2\text{D}^+/\text{HD}_2^+$ corresponds to the thermal value of the tandem mass spectroscopy given in Ref. 9. This observation verifies that the average energy of the reactant ions in an ICR cell in the single-resonance mode is thermal, as has been suggested in earlier work (Ref. 12).

References

1. Anders, L. R., et al., *J. Chem. Phys.*, Vol. 45, No. 1062, 1966.
2. Beauchamp, J. L., Anders, L. R., and Baldeschwieler, J. D., *J. Am. Chem. Soc.*, Vol. 89, No. 4569, 1967.
3. Baldeschwieler, J. D., *Science*, Vol. 159, No. 263, 1968.
4. Fluegge, R. A., "Symmetrical Charge Exchange and Ion Atom Reactions," Cornell Aeronautical Laboratory Report UA-1854-P-1. U. S. Department of Commerce Clearing House for Federal Scientific and Technical Information, Washington, D.C.
5. Gioumouisis, G., and Stevenson, D. P., *J. Chem. Phys.*, Vol. 29, No. 294, 1958.
6. Stevenson, D. P., and Schissler, D. O., *J. Chem. Phys.*, Vol. 29, No. 282, 1958.
7. Reuben, B. G., and Friedman, L., *J. Chem. Phys.*, Vol. 37, No. 1636, 1962.
8. Giese, C. F., and Maier, W. B., II, *J. Chem. Phys.*, Vol. 39, No. 739, 1963.
9. Futrell, J. H., and Abramson, F. P., "Ion Molecule Reactions in the Gas Phase," *Advan. Chem.*, Series 58, 1966.
10. Neynaber, R. H., and Trujillo, S. M., *Phys. Rev.*, Vol. 170, No. 0000, 1968.
11. Bowers, M. T., Elleman, D. D., and King, J., Jr., *J. Chem. Phys.*, Vol. 49, No. 0000, 1968.
12. Bowers, M. T., Elleman, D. D., and Beauchamp, J. L., *J. Phys. Chem.*, Vol. 72, No. 3599, 1968.
13. Anders, L. R., Ph.D thesis. Harvard University, Cambridge, Mass., 1966.
14. Beauchamp, J. L., *J. Chem. Phys.*, Vol. 46, No. 1231, 1967.
15. Beauchamp, J. L., and Buttrill, S. E., Jr., *J. Chem. Phys.*, Vol. 48, No. 1783, 1968.

B. Observation of Fluorine-19 Isotopic NMR Chemical Shifts Due to Chlorine-35 and Chlorine-37 Isotopes, E. A. Cohen and S. L. Manatt

I. Introduction

Isotopic substitution on an atom possessing a nuclear spin has been known for some time to cause changes of nuclear-magnetic-resonance (NMR) shieldings or chemical shifts (Ref. 1). The NMR shielding or chemical shift of a nucleus is defined as the extent to which the NMR field is increased by coupling between the nuclei and the electronic circulation induced by the applied magnetic field. The values of the chemical shift for a particular isotope in different chemical environments can vary tremendously and can be used to characterize very subtle features of local electronic structure.

Usually the NMR shielding of a nucleus in a particular chemical environment is highest when substituted with the heavier isotope of an isotopic pair (Ref. 1). Many examples of this effect on proton and fluorine shifts arising from substitution of a deuterium atom for a proton

have been described. Also, numerous examples of the proton and fluorine shifts caused by replacement of ^{12}C by ^{13}C have been reported (Ref. 1). Only a few examples of shifts have been observed for other heavier isotopes, such as ^{28}Si — ^{29}Si on ^{19}F , ^{32}S — ^{33}S on ^{19}F , ^{32}S — ^{34}S on ^{19}F , ^{80}Se — ^{76}Se — ^{77}Se — ^{78}Se — ^{82}Se on ^{19}F , ^{12}C — ^{13}C on ^{59}Co , and ^{14}N — ^{15}N on ^{59}Co (Ref. 1).

Only very approximate theories now exist for this effect in the case of molecules more complicated than the isotopic species of the hydrogen molecule (Ref. 1). Isotopic shifts most certainly arise from small differences in the average bond distances due to differences of molecular zero-point vibrational energies and anharmonic contributions to potential functions. A complete quantitative treatment of these effects would require accurate molecular wave functions, which are not yet available, and rather detailed knowledge of how these functions are affected by the various vibrational degrees of freedom of the isotopic species of a molecule. In general, the isotope chemical shift of a particular nucleus is proportional to the number of atoms in the molecule that have been isotopically substituted (Ref. 1). This article presents the first examples of chlorine isotope shifts on the fluorine-19 resonances in three molecules.

2. Fluorotrichloromethane Molecule

The fluorine-19 chemical shift of fluorotrichloromethane (CCl_3F) has for some time been used as the accepted chemical shift reference compound for fluorine-19 NMR (Ref. 2). Reference 3 states that, "A convenience reference signal is one which is sharp and well separated from other signals in the spectrum." It is common practice, and quite convenient at present, to utilize an internal reference (usually added to a sample subjected to NMR studies) as the control signal for locking the field and frequency of an NMR spectrometer. Such a control system is described in Ref. 4.

In Fig. 1a, the NMR spectrum of CCl_3F is exhibited along with that of hexafluorobenzene (C_6F_6) for a resolution reference. It is clearly evident that the signal from CCl_3F is a doublet, each member of which is significantly broader than the signal from C_6F_6 . The doublet nature of the CCl_3F signal explains why a noisy lock signal and poor resolution were obtained when, some time ago, an attempt was made to utilize the CCl_3F resonance as a control signal for field-frequency control of an NMR spectrometer having a magnet exhibiting very high field homogeneity. Apparently, rapid magnetic-field fluctuations and the close proximity of the two axis crossing

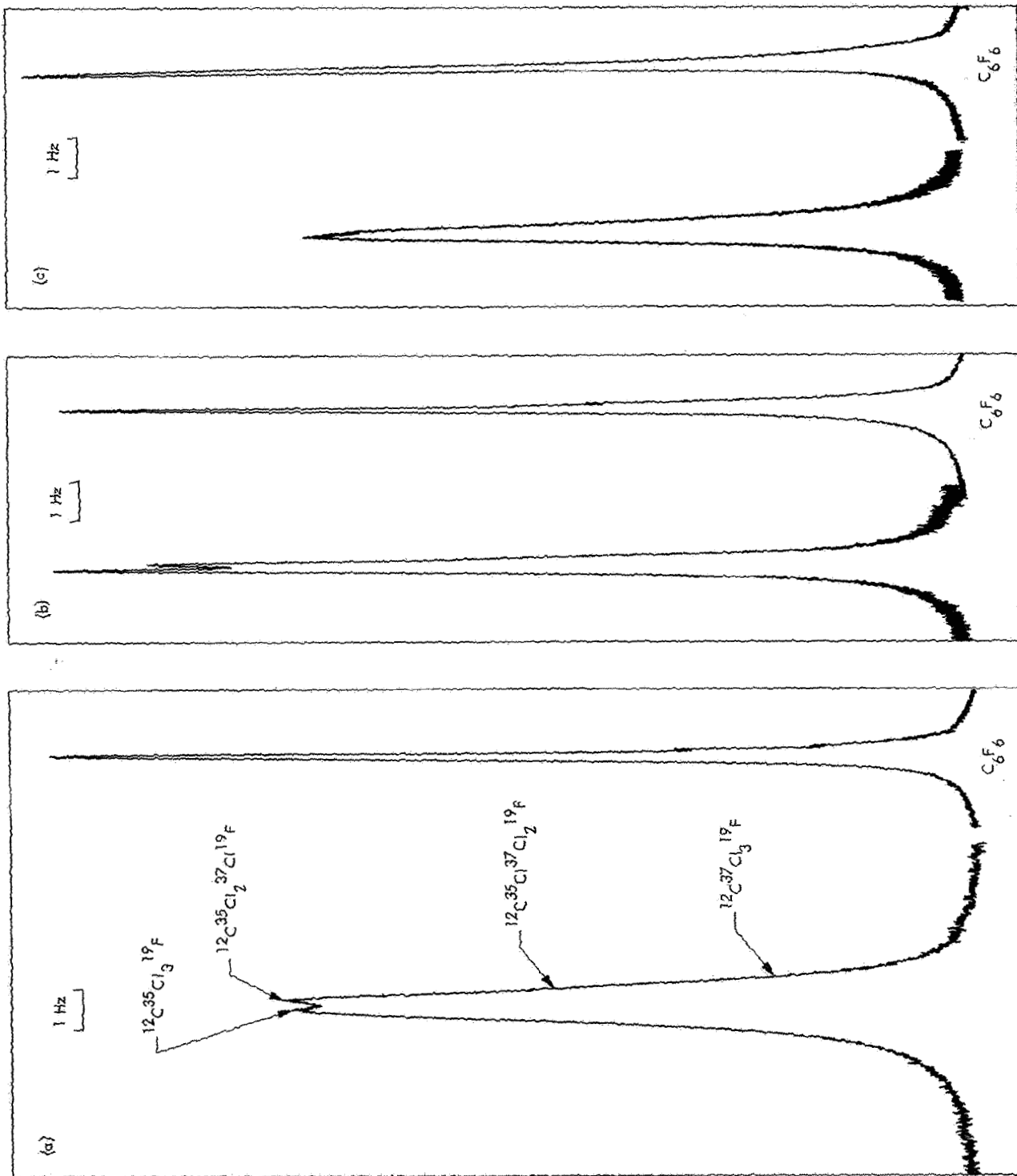


Fig. 1. Fluorine- ^{19}F spectra: (a) fluorotrichloromethane, (b) *cis*-1,2-difluorodichloroethylene, (c) *trans*-1,2-difluorodichloroethylene

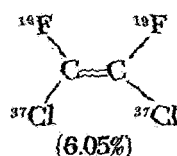
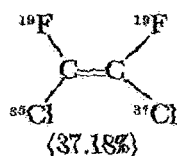
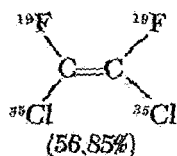
points of the derivative-like signal (from which the control signal to the magnet is derived) resulted in rapid jumping between the two possible stable control points.

The spectrum in Fig. 1a can be interpreted as exhibiting an isotope shift of 0.30 Hz at 56.4 MHz between the species $^{12}\text{C}^{35}\text{Cl}_3^{19}\text{F}$ and $^{12}\text{C}^{35}\text{Cl}_2^{37}\text{Cl}^{19}\text{F}$. Besides these two isotopic species, which should be present in 42.87% and 41.95%, respectively, the molecules $^{12}\text{C}^{35}\text{Cl}^{37}\text{Cl}_2^{19}\text{F}$ and $^{12}\text{C}^{37}\text{Cl}_3^{19}\text{F}$ are present to the extents of 13.69% and 1.49%, respectively. The low field peak of CCl_3F is interpreted as due to the $^{12}\text{C}^{35}\text{Cl}_3^{19}\text{F}$ species and the high field peak as due to the $^{12}\text{C}^{35}\text{Cl}_2^{37}\text{Cl}^{19}\text{F}$ species. The larger apparent intensity of the latter peak stems from the presence of the weaker unresolved peaks of $^{12}\text{C}^{35}\text{Cl}^{37}\text{Cl}_2^{19}\text{F}$ and $^{12}\text{C}^{37}\text{Cl}_3^{19}\text{F}$ species under the high field skirt of the $^{12}\text{C}^{35}\text{Cl}_3^{37}\text{Cl}^{19}\text{F}$ line.

The difference of linewidths between the CCl_3F species and C_6F_6 , most probably arises because chlorine-35 and chlorine-37 have nuclear spins greater than $\frac{1}{2}$. Such nuclei have electric quadrupole moments whose fast relaxation usually effectively decouples spin $> \frac{1}{2}$ nuclei from spin $= \frac{1}{2}$ nuclei when the electric-field gradients are large in the vicinity of the former nuclei (Ref. 5). The broadness of the CCl_3F signals suggests that, in this molecule, some residual spin-spin interaction exists between the chlorine nuclei and the fluorine because of relatively small electric-field gradients at the chlorine nuclei.

3. *cis*-1,2-Difluorodichloroethylene Molecule

In Fig. 1b, the fluorine-19 spectrum of *cis*-1,2-difluorodichloroethylene is shown. In this case, the following isotopic species are present in the abundances indicated:



The spectrum of this compound is interpreted as exhibiting a low field peak of relative intensity 0.57 and a higher field peak of intensity 0.37, with a peak intensity of 0.06 up-field and not resolved from the latter. In this molecule, the fluorines on a carbon atom with a chlorine-35 will all have the same chemical shift because of the effect of a chlorine-37 atom three bonds away (in the $^{19}\text{F}^{35}\text{Cl}^{12}\text{C}=\text{C}^{37}\text{Cl}^{19}\text{F}$ molecules) will be negligible.

For this compound one might expect to see two peaks with intensities of 0.754 and 0.246. However, the situation is slightly more complicated because, in the molecule $^{19}\text{F}^{35}\text{Cl}^{12}\text{C}=\text{C}^{37}\text{Cl}^{19}\text{F}$, the two fluorines have slightly different chemical shifts and the nuclear spin-spin coupling of 37.5 Hz between the two fluorines gives rise to a spectrum characteristic of a highly coupled AB spin system (Ref. 6). The separation between the two resolved peaks in Fig. 1b is 0.15 Hz. A calculation of an AB system with a coupling constant of 37.5 Hz and chemical shift of about 0.3 Hz, which was observed between $^{12}\text{C}^{35}\text{Cl}_3^{19}\text{F}$ and $^{12}\text{C}^{35}\text{Cl}_2^{37}\text{Cl}^{19}\text{F}$, indicates that the two center lines of such an AB spin system would only be 0.0024 Hz apart or, for all practical purposes, a singlet halfway between the chemical shift positions of the two nuclei. The observed 0.15-Hz separation then corresponds to one-half the isotope shift between the $^{19}\text{F}-^{12}\text{C}-^{35}\text{Cl}$ and $^{19}\text{F}-^{12}\text{C}-^{37}\text{Cl}$ fragments present in the species $^{19}\text{F}^{35}\text{Cl}^{12}\text{C}=\text{C}^{35}\text{Cl}^{19}\text{F}$ and $^{19}\text{F}^{35}\text{Cl}^{12}\text{C}=\text{C}^{37}\text{Cl}^{19}\text{F}$.

The spectral linewidths for *cis*-1,2-difluorodichloroethylene are significantly narrower than those for CCl_3F . This suggests that the local electric-field gradients must be significantly greater than in the former; thus, the chlorine isotopes' nuclear spins are more effectively decoupled from the fluorine nuclear spins by fast nuclear quadrupole relaxation.

4. *trans*-1,2-Difluorodichloroethylene Molecule

In the fluorine-19 spectrum of *trans*-1,2-difluorodichloroethylene shown in Fig. 1c, two things are evident: (1) The linewidths are significantly broader than those in the *cis*-isomer; and (2) the lineshape is indicative of unresolved multiplet structure.

One would expect that the isotope shift in this compound is similar in magnitude and nature to that observed in the *cis*-compound. The observed spectrum results from a single low field line from the all chlorine-35 species, a single line from a strongly coupled AB system ($J_{AA} \approx -129.6$ Hz) from the chlorine-35-chlorine-37 species one half the isotope shift up-field from the first line,

and a much weaker highest field line from the all chlorine-37 species. A complete lineshape analysis and studies at a higher magnetic field should confirm this. The broader linewidths in the *trans*-compound indicate that the electric field gradients experienced by the chlorine nuclei are significantly less (and much smaller) than those existing in the *cis*-compound.

5. Concluding Remarks

For the first time, the effect of chlorine isotopic substitution on fluorine-19 chemical shifts has been observed in three molecules. Also, from the fluorine linewidths in these three compounds, the relative magnitudes of electric-field gradients at the chlorine nuclei could be inferred. Because of its significant linewidth and apparent doublet structure, the unsatisfactory nature of CCl₃F as an internal reference signal for obtaining a nuclear stabilization signal for controlling NMR spectrometers and for referencing fluorine-19 NMR chemical shifts has been pointed out.

References

1. Batiz-Hernandez, H., and Bernheim, R. A., "The Isotope Shift," *Progress in Nuclear Magnetic Resonance Spectroscopy*, Vol. 3, p. 63. Edited by J. W. Emsley, J. Feeney, and L. H. Sutcliffe. Pergamon Press, London, 1967.
2. Filipovich, G., and Tiers, G. V. D., "Fluorine N.S.R. Spectroscopy. I. Reliable Shielding Values, ϕ , By Use of CCl₃F as Solvent and Internal Reference," *J. Phys. Chem.*, Vol. 63, No. 761, 1959.
3. Pople, J. A., Schneider, W. G., and Bernstein, H. J., *High-Resolution Nuclear Magnetic Resonance*, p. 78. McGraw-Hill Book Company, Inc., New York, 1959.
4. Elleman, D. D., Manatt, S. L., and Pearce, C. D., "Relative Signs of the Nuclear Spin Coupling Constants in Propylene Oxide and Indene Oxide," *J. Chem. Phys.*, Vol. 42, No. 650, 1965.
5. Abragam, A., *The Principles of Nuclear Magnetism*, Chap. VII, VIII, and XI. Oxford University Press, London.
6. Corio, P. L., "The Analysis of Nuclear Magnetic Resonance Spectra," *Chem. Rev.*, Vol. 60, No. 363, 1960.

C. An Energy-Level Iterative NMR Method for Sets of Magnetically Nonequivalent, Chemical Shift Equivalent Nuclei, S. L. Manatt, M. T. Bowers, and T. I. Chapman

1. Introduction

Nuclear magnetic resonance (NMR) spectroscopy has developed into one of the most useful tools for the chem-

ist's study of both dynamic properties, such as relaxation processes and conformational changes, and steady-state properties, such as stereochemistry and molecular structure. To extract the maximum information from the NMR spectrum of a system, it is usually necessary to accurately analyze complex NMR multiplet patterns. The eigenvalues of the high-resolution spin Hamiltonian

$$H = \sum_{i=1}^n h_i I_{zi} + \sum_{i < j}^n J_{ij} \mathbf{I}_i \cdot \mathbf{I}_j \quad (1)$$

must be obtained, thus yielding the chemical shifts h_i and the spin-spin coupling constants J_{ij} . In Eq. (1), \mathbf{I}_i is the total spin angular momentum of nucleus i and I_{zi} is the z -component of \mathbf{I}_i . The important parameters for the chemist that are obtained from NMR spectral analyses are h_i and J_{ij} . These parameters can be related directly to molecular configuration, molecular wave functions, intramolecular fields, and intermolecular fields.

The summations in Eq. (1) extend over all n nuclei and all unique pairs of nuclei in the first and second terms. If the number of nuclei is small, certain analytical solutions exist for the secular equations resulting from Eq. (1). From these closed expressions, the values of the h_i and J_{ij} may usually be obtained from a straightforward analysis of the experimental spectrum. The easily obtained analytical solutions are discussed in detail in Refs. 1-3.

As is most often the case, the experimental spectrum may result from a large number (≥ 4) of strongly coupled nuclei, and in this situation a simple analytical solution is not possible. The first attempts at analyzing these complex spectra utilized the trial-and-error method. Trial h_i and J_{ij} were guessed, and the resulting Hamiltonian matrix was diagonalized to yield an approximate set of energy levels and transition frequencies. This trial-and-error approach is laborious and inefficient and may result in spectral parameters of questionable accuracy.

When high-capacity, high-speed electronic computers became available, several investigators wrote iterative-type computer programs to reduce both the inaccuracy and the labor of retrieval of NMR parameters extracted from complex spectra. The programs most widely used are primarily the result of the initial work of J. D. Swalen and C. A. Reilly (Refs. 4 and 5) and R. A. Hoffman (Ref. 6). Both types of programs are reviewed here to facilitate understanding of the structure and utility of the method developed in the present work.

2. Swalen and Reilly (SR) Method

In the SR method, an approximate Hamiltonian matrix \mathbf{H}^0 is calculated from Eq. (1), using the spin product functions as a basis set and assumed values of the h_i and J_{ij} . The matrix elements are calculated by a straightforward application of the coupling properties of angular momentum (Refs. 1-3). The expectation value of the total spin component in the z -direction for a particular submatrix of energy levels is

$$\mathbf{F}_z = \sum_i^n I_{zi} \quad (2)$$

which commutes with \mathbf{H} . The matrix \mathbf{H}^0 is block diagonal in \mathbf{F}_z . The various \mathbf{F}_z blocks are then diagonalized using

$$\mathbf{S}^{-1} \mathbf{H}^0 \mathbf{S} = \Lambda^0 \quad (3)$$

with the columns of the transformation matrix \mathbf{S} corresponding to the individual eigenvalues of \mathbf{H}^0 . From the Λ_i^0 in Eq. (3), approximate allowed transition frequencies are obtained ($\Delta \mathbf{F}_z = \pm 1$) by

$$\nu_{ij}^0 = \Lambda_i^0 - \Lambda_j^0 \quad (4)$$

and the corresponding intensities are obtained in the usual manner (Refs. 1-3).

Using the approximate frequencies in Eq. (4), the experimental spectrum is assigned, and the iterative portion of the SR method is then used. From the observed transitions, the equations containing the n experimental energy levels can be written as

$$E_i - E_j = \nu_{ij}, \quad i = 1, 2, \dots, n-1, \quad i < j \quad (5)$$

If all n energy levels are connected by transitions, Eq. (5) can be solved for the E_i using the trace relationship

$$\sum_i^n E_i = 0 \quad (6)$$

Since it is usually possible to overdetermine the E_i from Eqs. (5) and (6), a least-squares method is used to solve for the E_i . The larger the number of transitions that can be assigned, the better the value of the E_i obtained. The program written by Swalen and Reilly for the above energy level analysis is called NMREN.

In certain cases, the rank of the energy level matrix resulting from the analysis of Eq. (5) is less than $n-1$,

and conditions in addition to Eq. (6) are needed to remove the resultant singularity. These singularities arise any time the Hamiltonian matrix is partitioned into two or more groups with no connecting off-diagonal elements and no allowed transitions between the groups. This is almost always the case when chemical shift equivalent, magnetically nonequivalent nuclei are present in the molecule to be analyzed.

Swalen and Reilly realize this singularity exists and propose that additional trace relationships similar to Eq. (6) could be included to correct the problem (Refs. 4 and 5). However, different trace relationships are needed for each distinct partitioning of the Hamiltonian matrix, and often the Hamiltonian matrix contains three or four such noncoupled subgroups. In addition, to avoid singularities it is necessary to assign enough transitions to couple all of the energy levels within each subgroup. Often this is very difficult or impossible. Again this lack of energy level coupling would require specific trace relationships for each such case encountered. The presentation of a general method for avoiding such singularities without using any trace relationship other than Eq. (6) is the main purpose of this article. A detailed account of the procedure is given in *Subsection 4*.

After the set of energy levels, termed Λ_{obs} , is obtained from the least-squares analysis of Eqs. (5) and (6), the approximate eigenvectors \mathbf{S} are used in a reverse transformation to obtain improved diagonal elements:

$$H_{ii} = (\mathbf{S} \Lambda_{\text{obs}} \mathbf{S}^{-1})_{ii} = \sum_k S_{ik}^2 E_k \quad (7)$$

The quantities

$$(H_{ii}^{(1)})^2 = (H_{ii} - \Lambda_i^0)^2 \quad (8)$$

are minimized, where the Λ_i^0 are the diagonal elements of the approximate Hamiltonian matrix \mathbf{H}^0 (derived in Eq. 3). Corrections to the parameters, Δh_i and ΔJ_{ij} , are calculated from the least-squares solution of Eq. (8), and the entire process is repeated. The iterative process is stopped after a set number of iterations or when the solution converges or diverges to a preset limit. Standard error analysis on the energy levels and final parameters is performed in the usual way (Refs. 4 and 5). The program that calculates \mathbf{H}^0 , diagonalizes \mathbf{H}^0 , and performs the iterative least-squares solution for the h_i and J_{ij} is called NMRIT. When used only to generate trial spectrum, it is designated NMRIT(0).

An extension of the SR method to include symmetry factoring of the Hamiltonian due to the presence of both chemically and magnetically equivalent nuclei has been carried out by R. C. Ferguson and D. W. Marquardt (Ref. 7). While this extension is very useful in handling large-spin systems containing many equivalent nuclei, it does not allow solution of the problems that arise from the chemically equivalent, magnetically nonequivalent nuclei mentioned above or those cases where not enough spectral lines can be assigned to relate all the energy levels within each symmetry subgroup of energy levels.

3. Hoffman Method

The Hoffman method (Ref. 6) is quite similar to the SR method. Hoffman decomposes the Hamiltonian matrix

$$\mathbf{H} = \mathbf{H}^0 + \mathbf{H}^{(1)} \quad (9)$$

into a zero-order component \mathbf{H}^0 , which is identical to that in Eq. (3), and a correction term $\mathbf{H}^{(1)}$. Diagonalization of \mathbf{H}^0 is performed as in Eq. (3), and the resulting transformation matrix is used to transform $\mathbf{H}^{(1)}$. The observed line frequencies ν_{ij} are related to ν_{ij}^0 , calculated from \mathbf{H}^0 , and $\nu_{ij}^{(1)}$ by

$$\nu_{ij}^{(1)} = \nu_{ij} - \nu_{ij}^0 \quad (10)$$

where

$$\nu_{ij} \cong (\mathbf{S}^{-1} \mathbf{H}^{(1)} \mathbf{S})_{ii} - (\mathbf{S}^{-1} \mathbf{H}^{(1)} \mathbf{S})_{jj} \quad (11)$$

From Eq. (11), a set of corrections, Δh_i and ΔJ_{ij} , to the h_i^0 and J_{ij}^0 can be obtained, and the entire process is repeated until a fit is obtained.

A method formally identical to that of Hoffman has been extensively developed by S. Castellano and A. A. Bothner-By (Ref. 8). With their method, Eq. (11) is solved using a least-squares technique. The structure of this program is such that the problem of chemical shift equivalent, magnetically nonequivalent sets of nuclei is treated by specifying the sets of spectral parameters which should be equally and synchronously varied.¹ This aspect of the method had not been succinctly stated when the present work was initiated.

4. Computational Method

The formalism of the method reported here closely follows that of the SR method given above. However,

¹Private communication with S. Castellano of Carnegie-Mellon University, Pittsburgh, Pa.

modifications were made to eliminate the necessity for submitting at least two separate programs for a single attempted fit of the observed spectrum, i.e., NMREN followed by NMRIT. If the energy level matrix is singular, for reasons discussed above, each sub-block of levels must be run separately as if it were a complete set of energy levels. Considerable hand calculation must then be performed to correct for the error in assuming Eq. (6) is valid for each sub-block. For a six-spin system, the hand calculations can require several hours for each run; for larger-spin systems, the time required becomes formidable. As mentioned above, an array of trace relationships could, in theory, be included to cover all possible contingencies. This would considerably complicate NMREN and would still leave NMREN isolated from NMRIT.

In the method described here, once an assignment is made, the experimental transitions are separated into connected groups and each group is treated automatically by NMREN-2. The partitioning into groups is arbitrary, and the initial number of groups has proven to have no effect on the values of the final parameters, in most cases, within experimental error. The only requirement on a group is that all energy levels within it be connected. The program then proceeds as in NMREN-2 and calculates a set of energy levels for each group of transitions.

Although the groups of levels are internally consistent, they are not zeroed properly relative to each other since Eq. (6) was assumed valid for each group. Correction to the proper zero is made as follows: The observed energy levels are stored on magnetic tape, and a set of approximate energy levels Λ_i^0 is calculated from assumed parameters and Eq. (3). The observed energy levels are recalled, and

$$\Delta_i^k = E_i^k - \Lambda_i^{k0} \quad (12)$$

is calculated. The indices i and k are the energy level and group index, respectively. The Δ values are then averaged:

$$\langle \Delta^k \rangle = \frac{1}{N} \sum_{i=1}^N \Delta_i^k \quad (13)$$

where N is the number of energy levels in group k . The $\langle \Delta^k \rangle$ are closely approximated by

$$\langle \Delta^k \rangle \cong \frac{1}{N} \sum_{i=1}^N E_i^k \quad (14)$$

and hence yield the correction factor necessary to compensate for the assumption of the validity of Eq. (6) for each group.

This program, termed NMRENIT, then proceeds to calculate the corrected set of observed energy levels

$$E_i^{k'} = E_i^k \pm |\langle \Delta^k \rangle| \quad (15)$$

where the plus sign holds if $\langle \Delta^k \rangle$, calculated from Eq. (13), is negative and the minus sign holds if $\langle \Delta^k \rangle$ is positive. The program then orders the $E_i^{k'}$ to correspond to the $\Lambda_i^{k_0}$, and an iterative procedure identical to NMRIT is followed. After each iteration, the above correction procedure is repeated to adjust for any errors in Eq. (14) and to assure that the $E_i^{k'}$ remain properly labeled relative to the $\Lambda_i^{k_0}$. Limitation of the number of iterations and calculation of the errors in the parameters are identical to those for the NMRIT case.

The operations of the NMRENIT program can be summarized by the following seven steps, using Fig. 2, which is similar to the schematic diagram presented in Ref. 4:

- (1) The energy level matrix Λ_{obs}^k for each of the k groups is calculated from the assigned $(v_{ij}^k)_{\text{obs}}$.

- (2) \mathbf{H}_{calc} is calculated from the trial parameters h_i and J_{ij} .
- (3) \mathbf{H}_{calc} is diagonalized to give the diagonal matrix Λ_{calc} and the corresponding approximate eigenvector matrix \mathbf{S} .
- (4) Λ_{obs} is obtained from the Λ_{obs}^k using Λ_{calc} and the averaging and ordering technique discussed above.
- (5) Λ_{obs} is reverse-transformed using the approximate eigenvectors \mathbf{S} to yield an approximate observed Hamiltonian \mathbf{H}_{obs} .
- (6) The diagonal elements of \mathbf{H}_{obs} are used along with Λ_{calc} to calculate changes in the trial h_i and J_{ij} by the least-squares technique indicated above. [Steps (2-6) are repeated until a convergent solution is reached or until a preset number of iterations has been completed.]
- (7) The v_{ij} and the corresponding intensities are computed from the final Λ_{calc} and \mathbf{S} . The v_{ij} are compared with the $(v_{ij}^k)_{\text{obs}}$ with an output format identical to that of NMRIT.

Thus, two separate programs, NMREN-2 and NMRIT, are no longer necessary when using the SR method

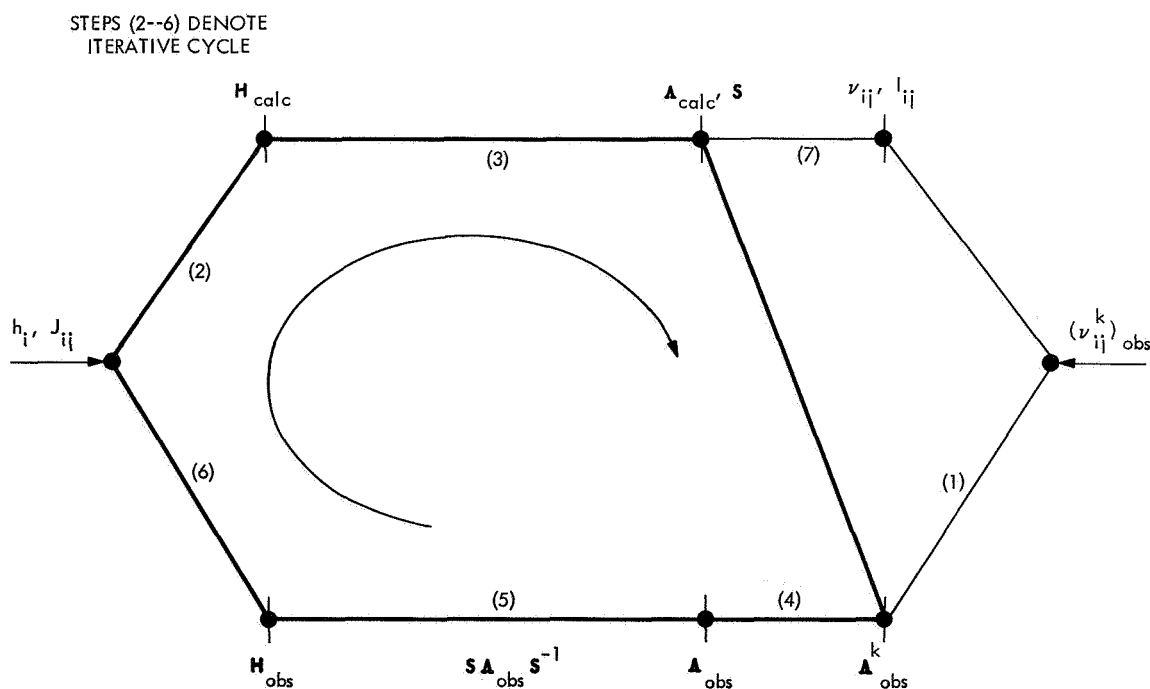


Fig. 2. Operations of the NMRENIT program

(Refs. 4 and 5); instead, programs similar to NMREN-2 and NMRIT are used as subroutines in a master program termed NMRENIT. Hand calculations and data transfer of NMREN-2 results are no longer required. It is no longer necessary to run a separate NMREN program for each subgroup of connected energy levels; instead, a single input carries the problem to an iterative solution. The present program greatly facilitates the energy level iterative analyses of spin systems possessing sets of magnetically nonequivalent, chemical shift equivalent nuclei. The methods that accomplish the latter also allow for the first-time attainment of convergent iterative solutions based on fewer spectral transitions than are necessary to link all the energy levels in a particular symmetry group (provided each energy level is represented at least once). Naturally, the more transitions that can be assigned, the better the value of the E_i^k obtained, but adequate fits have been obtained from a minimum number.

Finally, the methods of the present program, although limited for the moment to eight-spin systems, were conceived allowing for their possible extension to more complex spin systems, perhaps through incorporation of the features of the equivalence factoring approach (Ref. 7) and/or with computers possessing larger storage. The program NMRENIT was fit into an IBM 7094 computer using overlay techniques. The running time of NMRENIT using the JPL IBM 7094 computer system is 2 to 3 min for 10 iterations on a six-spin AA'BB'CC' system.

References

1. Pople, J. A., Schneider, W. G., and Bernstein, H. J., *High Resolution Nuclear Magnetic Resonance*. McGraw-Hill Book Company, Inc., New York, 1959.
2. Emsley, J. W., Feeney, J., and Sutcliffe, L. H., *High Resolution Nuclear Magnetic Resonance Spectroscopy*. Pergamon Press, New York, 1965.
3. Corio, P. L., *Structure of High-Resolution NMR Spectra*. Academic Press, New York, 1966.
4. Swalen, J. D., and Reilly, C. A., "Analysis of Complex NMR Spectra. An Iterative Method," *J. Chem. Phys.*, Vol. 37, No. 21, 1962.
5. Reilly, C. A., and Swalen, J. D., "Nuclear Magnetic Resonance of Some Simple Epoxides," *J. Chem. Phys.*, Vol. 32, No. 1378, 1960.
6. Hoffman, R. A., "Analysis of High-Resolution NMR Spectra by Iterative Methods," *J. Chem. Phys.*, Vol. 33, No. 1256, 1960.
7. Ferguson, R. C., and Marquardt, D. W., "Computer Analysis of NMR Spectra: Magnetic Eigenvalence Factoring," *J. Chem. Phys.*, Vol. 41, No. 2087, 1964.
8. Castellano, S., and Bothner-By, A. A., "Analysis of NMR Spectra by Least Squares," *J. Chem. Phys.*, Vol. 41, No. 3863, 1964.

D. Exterior Forms and General Relativity,

F. B. Estabrook and T. W. J. Unti

When a physical theory is formulated as a coupled set of first-order partial differential equations, the existence of "general solutions" of the set can immediately be discussed using the results of E. Cartan (Ref. 1). When other, so-called "particular" classes of solutions can be found, they too may similarly, but separately, be discussed and classified.

The method consists of recasting the problem to that of finding certain integral surfaces of closed systems of exterior differential forms in a space of n dimensions, where $n - p$ is the number of dependent variables and p the number of independent variables of the original partial differential set. The integral surfaces sought are submanifolds of dimensions p or less; in the p -dimensional integral manifolds, the independent variables may vary freely. The general solutions of the original set are those integral manifolds of dimension p that contain, at every point, integral elements of dimension $p - 1$, which in turn contain integral elements of dimension $p - 2$, etc. The existence criteria for such general solutions have been derived by Cartan through systematic use of the Cauchy-Kowalewski theorem; i.e., these criteria may, in principle, be obtained by integration from suitably set boundary conditions on manifolds of dimension $p - 1$.

Cartan gives a systematic procedure for first calculating a set of "reduced characters," integers $s'_0, s'_1, \dots, s'_{p-1}$, and then comparing the integer

$$ps'_0 + (p - 1)s'_1 + \dots + s'_{p-1}$$

to the number of constraints, h , that relate the differentials of the dependent variables in the p -dimensional integral manifolds. (In the present case, h is just the original number of first-order partial differential equations.) If these are equal, the set is said to be "in involution," and the general solution exists; in a Cauchy integration from conditions on an arbitrary $(p - 1)$ -dimensional boundary, precisely

$$s'_p \equiv n - p - s'_0 - s'_1 - \dots - s'_{p-1}$$

functional relationships (between the independent and dependent variables) may still be arbitrarily imposed to achieve a unique solution.

Here, the property of being "in involution" is regarded as a requirement for a well-set physical theory. As a first example, Maxwell's equations *in vacuo* become two 3-form equations:

$$\begin{aligned}
& [dE_x dx dt] + [dE_y dy dt] + [dE_z dz dt] \\
& + [dB_x dy dz] + [dB_y dz dx] + [dB_z dx dy] = 0 \\
& [dB_x dx dt] + [dB_y dy dt] + [dB_z dz dt] \\
& - [dE_x dy dz] - [dE_y dz dx] - [dE_z dx dy] = 0
\end{aligned}$$

with $n = 10$ and $p = 4$. The reduced characters are $s'_0 = 0$, $s'_1 = 0$, $s'_2 = 2$, $s'_3 = 4$, $h = 8$, and the system is in involution. Since $s'_4 = 0$, suitably set boundary conditions on a general bounding 3-dimensional manifold such as $t = \text{constant}$ serve uniquely to determine a solution through some range of t . (Characteristic 3-surfaces may also be treated by Cartan's methods.)

The dyadic equations for general relativity (Ref. 2) may be similarly analyzed. They have been found to be expressible as six 2-form equations and six 3-form equations. Only the terms in these involving the differentials of the dependent variables are included here; the terms involving forms that are products of the basis forms of independent variables (denoted by $\bar{\omega}_1, \bar{\omega}_2, \bar{\omega}_3, \bar{\omega}_4$) all have coefficients that are quadratic functions of the dependent variables, and can, when necessary, be read off from the original dyadic formulation. (Knowing already that the set is closed, only the structure of the terms involving differentials of the dependent variables is required for calculation of the reduced characters.) The 2-forms $d\bar{\omega}_1, d\bar{\omega}_2, d\bar{\omega}_3, d\bar{\omega}_4$ can similarly be obtained from the dyadic commutation relationships for \mathbf{D} and differentiations with respect to time:

$$\begin{aligned}
& [dN_{1i} \bar{\omega}_1] + [dN_{2i} \bar{\omega}_2] + [dN_{3i} \bar{\omega}_3] - [d\omega_i \bar{\omega}_4] = \dots \\
& [d\bar{S}_{1i} \bar{\omega}_1] + [d\bar{S}_{2i} \bar{\omega}_2] + [d\bar{S}_{3i} \bar{\omega}_3] + [da_i \bar{\omega}_4] = \dots \\
& [dB_{i1}^* \bar{\omega}_1 \bar{\omega}_4] + [dB_{i2}^* \bar{\omega}_2 \bar{\omega}_4] + [dB_{i3}^* \bar{\omega}_3 \bar{\omega}_4] \\
& + [dP_{1i} \bar{\omega}_2 \bar{\omega}_3] + [dP_{2i} \bar{\omega}_3 \bar{\omega}_1] + [dP_{3i} \bar{\omega}_1 \bar{\omega}_2] = \dots \\
& [dQ_{i1} \bar{\omega}_1 \bar{\omega}_4] + [dQ_{i2} \bar{\omega}_2 \bar{\omega}_4] + [Q_{i3} \bar{\omega}_3 \bar{\omega}_4] \\
& - [dB_{i1}^* \bar{\omega}_2 \bar{\omega}_3] - [dB_{i2}^* \bar{\omega}_3 \bar{\omega}_1] - [dB_{i3}^* \bar{\omega}_1 \bar{\omega}_2] = \dots
\end{aligned}$$

where

$$\bar{\mathbf{S}} = \mathbf{S} - \boldsymbol{\Omega} \times \mathbf{I}$$

$$i = 1, 2, 3$$

with $n = 48$ and $p = 4$, $s'_0 = 0$, $s'_1 = 6$, $s'_2 = 12$, $s'_3 = 14$, and $h = 8$. The system is in involution; $s'_4 = 12$ arbitrary functions may be chosen to determine a unique general solution.

Particular solutions are especially important in non-linear problems, since they may provide simpler sub-cases for study. For these, adding a number of further algebraic requirements does not reduce s'_4 by an equal number. For example, adding to the above the requirements for vacuum, which are 10 additional constraints ($\mathbf{T} = 0$, $\mathbf{t} = 0$, $\rho = 0$), gives a new involutory set for which $s'_4 = 6$. Adding further the nine requirements for a gaussian reference frame ($\mathbf{a} = 0$, $\boldsymbol{\Omega} = 0$, $\boldsymbol{\omega} = 0$) gives again an involutory set, for which $s'_4 = 0$. This is the discovery upon which so-called canonical formulations of general relativity are based.

This method has been used to analyze the dyadic equations for a case where the following are imposed: (1) vacuum, (2) axial symmetry, and (3) the compatible assumptions that $\dot{\mathbf{N}} + \mathbf{S}^* \cdot \mathbf{N} = 0$, $\mathbf{E} = 0$, and $\boldsymbol{\Omega} = 0$. Since *no* stationary or static condition has been assumed, there are three independent variables described by forms $\bar{\omega}_1, \bar{\omega}_2, \bar{\omega}_3$.

In fact, with

$$\mathbf{S} = \begin{pmatrix} 0 & 0 & 0 \\ 0 & \beta & \delta \\ 0 & \delta & \gamma \end{pmatrix}$$

$$\mathbf{N} = \begin{pmatrix} 0 & 0 & 0 \\ -\phi & 0 & 0 \\ \chi & 0 & 0 \end{pmatrix}$$

$$\mathbf{a} = (0, r, s)$$

$$\boldsymbol{\omega} = (p, 0, 0)$$

the following set of forms (or the equivalent set of partial differential equations) is shown, by lengthy calculation, to be *closed* (i.e., to have no further integrability

conditions):

$$\beta\gamma - \delta^2 = 0$$

$$[d\phi \bar{\omega}_1] - [d\chi \bar{\omega}_2] + (\phi^2 + \chi^2) [\bar{\omega}_1 \bar{\omega}_2] \\ + (-\beta\phi + \delta\chi - p\chi) [\bar{\omega}_1 \bar{\omega}_3] + (\gamma\chi - \delta\phi - p\phi) [\bar{\omega}_2 \bar{\omega}_3] = 0$$

$$[d\beta \bar{\omega}_1] + [d\delta \bar{\omega}_2] + [dr \bar{\omega}_3] + (\beta\phi - \gamma\phi - 2\delta\chi) [\bar{\omega}_1 \bar{\omega}_2] \\ + (-s\phi + r^2 + 2p\delta - \theta\beta) [\bar{\omega}_1 \bar{\omega}_3] \\ + (s\chi + rs - p\beta + p\gamma - \theta\delta) [\bar{\omega}_2 \bar{\omega}_3] = 0$$

$$[d\delta \bar{\omega}_1] + [d\gamma \bar{\omega}_2] + [ds \bar{\omega}_3] + (-\gamma\chi + \beta\chi + 2\delta\phi) [\bar{\omega}_1 \bar{\omega}_2] \\ + (r\phi + rs + p\gamma - p\beta - \theta\delta) [\bar{\omega}_1 \bar{\omega}_3] \\ + (-r\chi + s^2 - 2p\delta - \theta\gamma) [\bar{\omega}_2 \bar{\omega}_3] = 0$$

$$[dp \bar{\omega}_3] + (rp + r\delta - \beta s) [\bar{\omega}_1 \bar{\omega}_3] \\ + (sp - s\delta + \gamma r) [\bar{\omega}_2 \bar{\omega}_3] = 0$$

where $\theta = \beta + \gamma$. There is one 0-form equation, three 1-form equations derived from it (not included here), and four 2-form equations. With $n = 11$ and $p = 3$, $s'_0 = 1$, $s'_1 = 4$, $s'_2 = 3$, $h = 14$, the system is in involution, and $s'_3 = 0$.

The forms spanning the space of independent variables fulfill

$$d\bar{\omega}_1 = -\phi [\bar{\omega}_1 \bar{\omega}_2] + (p + \delta) [\bar{\omega}_2 \bar{\omega}_3] - \beta [\bar{\omega}_3 \bar{\omega}_1] \\ d\bar{\omega}_2 = \chi [\bar{\omega}_1 \bar{\omega}_2] + \gamma [\bar{\omega}_2 \bar{\omega}_3] + (p - \delta) [\bar{\omega}_3 \bar{\omega}_1] \\ d\bar{\omega}_3 = -s [\bar{\omega}_2 \bar{\omega}_3] + r [\bar{\omega}_3 \bar{\omega}_1]$$

These are, in form language, the commutation relationships of the usual dyadic operators, ∇ and (\cdot) , applied to scalars; $\bar{\omega}_1$ is radial, $\bar{\omega}_2$ expresses a co-latitude direction, and $\bar{\omega}_3$ is timelike. The unique solution is, in principle, now a matter of straightforward integration. Whether it can be found in closed form, however, is not yet known. The hope is that any such axial, non-static, vacuum solution can be of importance in the study and understanding of gravitational radiation. The assumptions of the present case would make the physical interpretation of any solutions especially easy, inasmuch as there is always present a one-parameter family of imbedded flat, Euclidean 3-spaces.

References

1. Cartan, É., *Les Systèmes Différentiels Extérieurs et Leurs Applications Géométriques*. Hermann et Cie., Paris, 1945.
2. Estabrook, F. B., and Wahlquist, H. D., Dyadic Analysis of Space-Time Congruences, *J. Math. Phys.*, Vol. 5, pp. 1629-1644, 1964.